

# The Low Frequency Array and Clusters of Galaxies

Namir Kassim,<sup>1,2</sup> Aaron Cohen,<sup>2,3</sup> and T. Joseph W. Lazio<sup>2</sup>

<sup>1</sup> *LOFAR Project Scientist*

<sup>2</sup> *Remote Sensing Division, Naval Research Laboratory, Washington, DC* and

<sup>3</sup> *National Research Council, Washington, DC*

We present an overview of the Low Frequency Array (LOFAR) project. LOFAR is intended to be a low frequency instrument ( $\nu \sim 10$  to 240 MHz) with massive collecting area ( $\sim 10^6$  m<sup>2</sup>) and high resolution ( $\sim 1''.5$  at 100 MHz). We discuss the major design concepts for LOFAR as well as the scientific motivation, with special emphasis on cluster research.

## 1. Introduction

The science of radio astronomy started at low frequencies with the discovery of celestial radio waves by K. Jansky at 20.5 MHz (Jansky 1935). However, below 150 MHz, large phase distortions introduced by the ionosphere have prevented the kind of high resolution, thermal noise limited images possible at higher frequencies.

The paucity of large aperture, high-sensitivity, synthesis instruments operating below 150 MHz means that this portion of the radio spectrum has been explored particularly poorly, despite the large number of astrophysical phenomena that can be addressed only by a sensitive, high-angular-resolution, low-frequency telescope:

- Continuum spectra over much larger frequency dynamic ranges for studies of shock acceleration and spectral aging in Galactic (supernova remnants) and extragalactic (radio galaxies and galaxy cluster relics) sources;
- Efficient detection of large numbers of steep spectrum sources, which can be imaged in some cases, including high-redshift radio galaxies, shocks driven by infalling matter in clusters of galaxies, and pulsars in the Milky Way and possibly in external galaxies;
- Probing the ionized interstellar medium (ISM) via measurements of radio wave scattering, the distribution of low density ionized gas toward nonthermal sources, and hydrogen and carbon recombination line observations of very high Rydberg state atoms;
- The large opacity of H II regions below 100 MHz can enable distance determinations to various foreground objects, in both the Galaxy and external galaxies, from which the three-dimensional distribution and spectrum of cosmic-ray emissivity can be determined as well as being used to measure their emission measures, temperatures, pressures, and ionization states

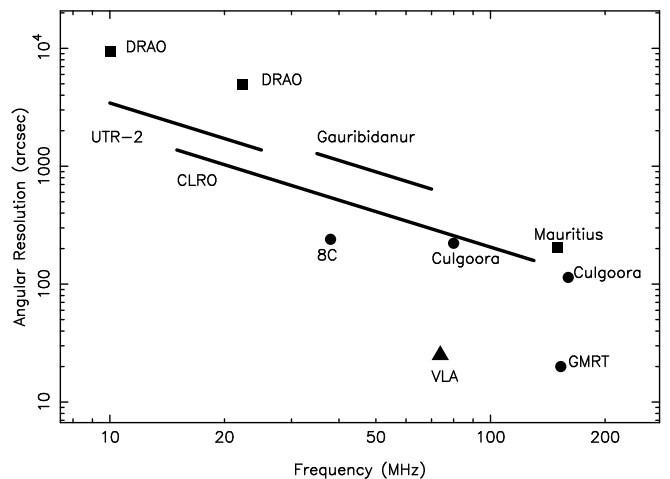


FIG. 1.— Resolution of the 74 MHz VLA as compared to other low frequency telescopes and surveys.

- Detection of coherent emission from sources such as the Sun, Jupiter, pulsars, and possibly radio bursts from nearby stars and extrasolar planets.

## 2. The Low Frequency VLA

The development of self-calibration has led to a revolution in low frequency radio interferometry, by finally permitting correction to previously intractable ionospheric phase effects. This permitted development of the 74 MHz system at the Very Large Array (VLA) telescope in Socorro, New Mexico (Kassim et al. 1993, 2003a). The first low-frequency ( $< 100$  MHz) system with long ( $> 10$  km) baselines, this system represents a major advance in both resolution and sensitivity in this frequency range (Figs. 1 and 2).

The 74 MHz VLA system has, in its short existence, already produced a wide variety of unique observations in a wide range of fields. Observation targets include clusters of galaxies (Fig. 3), radio galaxies (Fig. 4), normal galaxies, the Galactic Center, supernova remnants, H II regions, pulsars, the ISM and extrasolar planets. With increased computational power and the introduction of new data reduction techniques for radio frequency

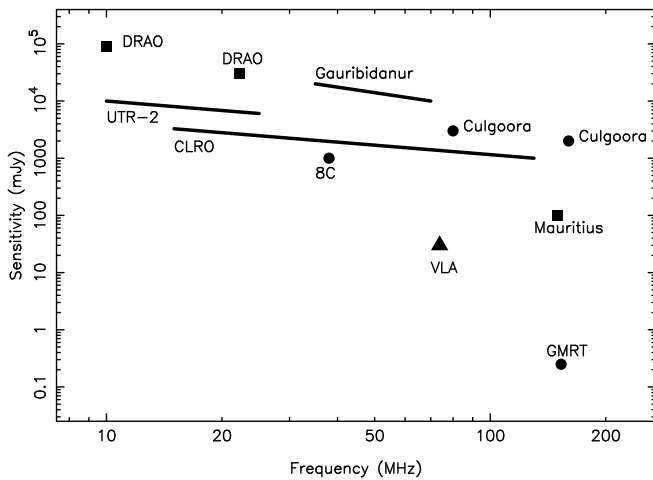


FIG. 2.— Sensitivity of the 74 MHz VLA as compared to other low frequency telescopes and surveys.

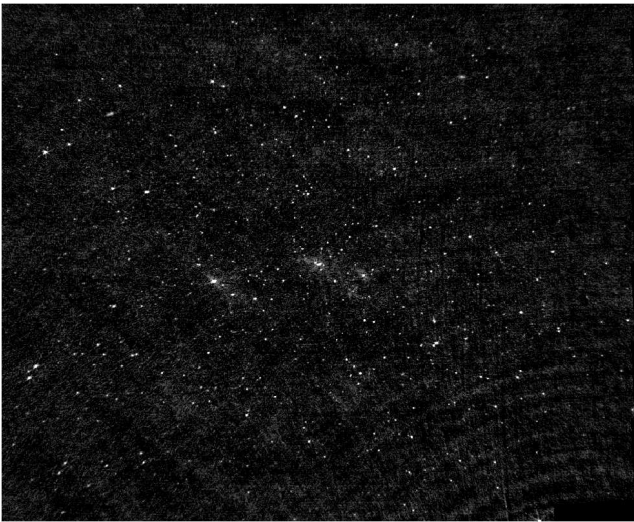


FIG. 3.— The Coma cluster of galaxies at 74 MHz (Kronberg 1999). This image shows the entire primary beam of the VLA at 74 MHz and illustrates the efficiency with which large sections of the sky can be imaged with a sensitive, long-wavelength instrument. The rms noise is  $25 \text{ mJy beam}^{-1}$ , and the field covers approximately  $15^\circ$  at a resolution of  $1'$ . The sidelobes apparent in the lower right section of the image result from insufficient CLEANing of the radio galaxy Virgo A, approximately  $20^\circ$  away. The Coma cluster of galaxies and its halo are in the central portion of the image.

interference (RFI) excision, ionospheric calibration, and wide-field imaging, both the 74 and 330 MHz VLA systems (the latter completed in 1990) have ushered in a quiet renaissance in low frequency radio astronomy.

### 3. LOFAR: Design Concept

The 74 MHz VLA system (Kassim et al. 1993, 2003a), with its unprecedented angular resolution ( $\approx 20''$ ), has unprecedented sensitivity ( $\approx 30 \text{ mJy beam}^{-1}$ ), even though its collecting area ( $\sim 10^3 \text{ m}^2$ ) is relatively modest. Its dramatic successes provide a strong incentive to develop a much larger ( $\sim 500 \text{ km}$  baselines) and more sensitive ( $A_{\text{eff}} > 10^5 \text{ m}^2$ ) instrument. Such an

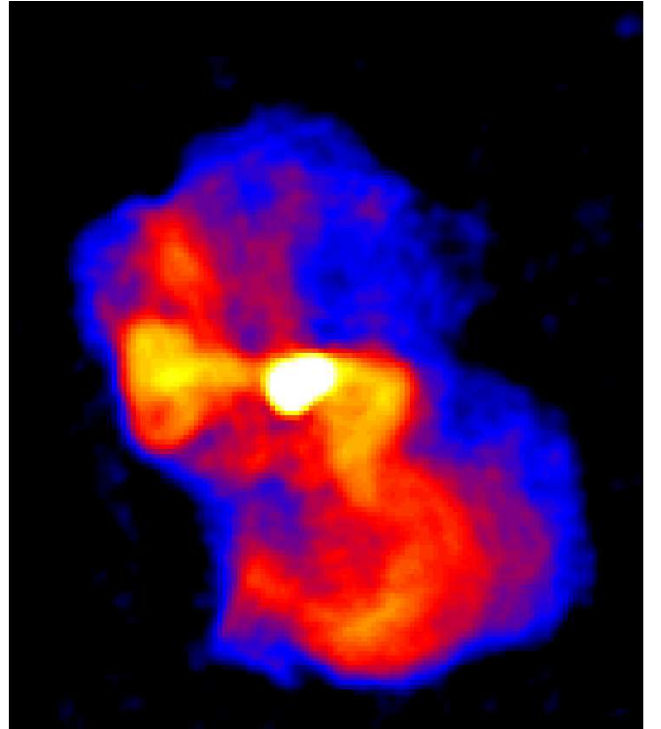


FIG. 4.— Virgo A at 74 MHz (Kassim et al. 1993). This image has an angular resolution of  $25''$  and is approximately  $15'$  in size. While sufficient to resolve the well-known radio halo of this active galaxy, detailed observations of the galaxy itself require higher angular resolution.

instrument could explore the entire low frequency radio spectrum at unmatched levels of sensitivity (sub-mJy) and angular resolution (arc-second) (Kassim & Erickson 1998; Kassim et al. 2003a) and will provide a unique and efficient tool both for large-scale emission studies (e.g., supernova remnants, the inner Galaxy, and galaxy and cluster halos), for high-sensitivity observations of small-diameter steep-spectrum sources (e.g., pulsars, high redshift radio galaxies, and extrasolar planets), and ionospheric and magnetospheric physics investigations.

Because the effective area of a dipole receiver is proportional to  $\lambda^2$ , at low frequencies, significant collecting area can be achieved with simple dipoles, without the need for expensive radio dishes. Thus, rather than an array of radio dishes, the strategy is to use “stations” each consisting of roughly 200 phased active dipole antennas spread over a roughly 100 meter circle on the ground (Fig. 5). Each station will function as a single antenna in an array such as the VLA. LOFAR will consist of roughly 100 stations, with baselines up to 500 km.

### 4. LOFAR: Technical Specifications

Motivated by the general design concept and the science goals outlined above, a series of scientific and technical requirements were developed to drive the LOFAR design. Table 1 summarizes the current technical specifications that emerged from those considerations.

**A New Spectral Window** The scientific projects described above, and serendipity, are all enhanced



FIG. 5.— Artist’s conception for the design of a LOFAR station.

TABLE 1. LOFAR BASIC SPECIFICATIONS

Parameter	Design Goal
Frequency Range	
Low	10–90 MHz <sup>a</sup>
High	110–240 MHz
Redshift Coverage (H I)	> 4.9
Effective Collecting Area	
Low (10–90 MHz)	$10^{6.1} (\nu/15 \text{ MHz})^{-2} \text{ m}^2$
High (110–200 MHz)	$10^{5.1} \text{ m}^2$
High (200–240 MHz)	$10^{5.1} (\nu/200 \text{ MHz})^{-2} \text{ m}^2$
Baselines	0.02–400 km
Angular Resolution (FWHM)	$0''.64$ at 240 MHz
Number of Receptors	
Low (10–90 MHz)	13,365 dipoles
High (110–240 MHz)	213,840 dipoles
Number of Stations	$\simeq 100$
Point Source Sensitivity <sup>b</sup>	
10 MHz	3.0 mJy
30 MHz	1.6 mJy
75 MHz	1.0 mJy
120 MHz	0.13 mJy
200 MHz	0.03 mJy
Brightness Temperature Sensitivity	
10 MHz	$10^{5.3} \text{ K}$
30 MHz	$10^{5.1} \text{ K}$
75 MHz	$10^{4.6} \text{ K}$
120 MHz	$10^{4.0} \text{ K}$
200 MHz	$10^{3.4} \text{ K}$
Instantaneous Sky Coverage	0.1 sr/beam at 10 MHz
Mapping Capability	Full field of view
Number of independent fields of view	8
Time Resolution	1 ms
Polarization	full Stokes

<sup>a</sup>LOFAR may include the 90–110 MHz band.

<sup>b</sup>Sensitivity calculations are for a single polarization, 1 hour integration, and 4 MHz bandwidth.

by an instrument that is as broad-band as possible within reasonable economic constraints. LOFAR should be capable of observing at as low a frequency as possible above the ionospheric cutoff near 10 MHz. Past experience has indicated that ionospheric scintillations, which cannot be removed by self-calibration, will degrade a non-negligible fraction of the data below roughly 30 MHz. Thus, we plan for an instrument which can reach 5 MHz, with a realization that it will operate with reduced efficiency below 30 MHz. At the upper end of its frequency range, LOFAR should reach the lower frequencies of other sensitive radio interferometers like the GMRT and the VLA. Based on these considerations, and driven also by the desire for a capability to detect red-shifted H I near  $z \sim 6$ , LOFAR’s upper frequency is at 240 MHz.

**Imaging** Poor angular resolution is the single greatest reason for the limited scientific yield of previous low radio frequency instruments. LOFAR should be capable of resolving radio galaxies, which have a median angular diameter of  $10''$ , at least at the higher end of LOFAR’s frequency range, and it should be able to conduct interstellar scattering observations with a resolution competitive to that employed by centimeter-wavelength VLBI ( $\approx 5 \text{ mas}$  at 1.4 GHz). However, previous low-frequency VLBI measurements (Clark et al. 1975) have shown that few sources have compact structures that can be detected on baselines longer than 500 km. A reasonable goal is an array whose longest dimensions are 400–500 km, producing approximately  $10''$  ( $1''$ ) resolution at 15 MHz (150 MHz) (Figure 6).

**Sensitivity** LOFAR should be competitive with centimeter-wavelength instruments for observations of moderately steep-spectrum sources. Earlier work on expanding the low frequency capabilities of the VLA (Perley & Erickson 1984) indicates that if the individual “stations” have effective areas  $A_{\text{eff}} \sim 10^3 \text{ m}^2$  at 74 MHz, the confusion and thermal-noise contributions to the system temperature are comparable. With a total collecting area of  $10^6 \text{ m}^2$  at 15 MHz, LOFAR could achieve milliJansky-level sensitivity in reasonable integration times, e.g., 0.5–1 mJy at 74 MHz for an 8-hour integration and 3 MHz bandwidth. The Expanded VLA (EVLA) will attain an point-source sensitivity of  $3.3 \mu\text{Jy}$  in 8 hr at 1400 MHz, so that observations of sources with spectra steeper than  $-1.3$  will be more effective with LOFAR. As the sensitivity (collecting area) of a sparse dipole array scales as  $\lambda^2$ , LOFAR’s projected sensitivity will also match smoothly to that of the GMRT at LOFAR’s high-frequency end ( $> 150 \text{ MHz}$ ) (Figure 6).

**Frequency Versatility** In order to constrain emission mechanisms for various classes of sources as well as distinguish between emission and absorption processes along the line of sight to a source, LOFAR

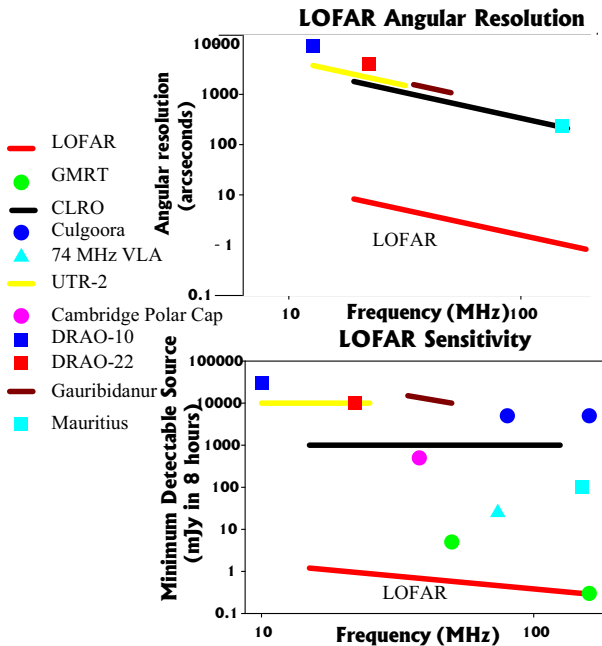


FIG. 6.— Angular Resolution and Sensitivity of LOFAR as compared to other past, present, and proposed imaging instruments in the 10–200 MHz range. The LOFAR sensitivity calculation is based on a  $\lambda^2$ -dependent collecting area assumed to be  $10^6 \text{ m}^2$  at 15 MHz. A bandwidth of 3 MHz and integration time of 8 hours have also been assumed. In both panels, in addition to LOFAR, the angular resolution and point-source sensitivity of the CLRO, Culgoora, 74 MHz VLA, UTR2, Cambridge Polar cap survey, DRAO-10 and DRAO-22, Gauribidanur, Mauritius, and GMRT are shown.

must be a broad-band instrument. Continuous frequency coverage, or as nearly continuous as allowed by interference, is required over LOFAR’s frequency range.

### Solar System and Space Weather Studies

LOFAR is anticipated to study solar nonthermal and thermal phenomena, e.g., flares and storms. LOFAR can also be used in conjunction with a separate transmitting facility to test the feasibility of using solar radar for studying coronal mass ejections (CMEs) and geomagnetic storm prediction, and for other solar, ionospheric, and space-weather applications. Therefore, LOFAR must have high time resolution, high surface-brightness sensitivity, and good instantaneous  $u$ - $v$  coverage.

**Spectroscopy** LOFAR should be able to study emission and absorption lines of carbon and other elements from the cold ISM. Therefore, LOFAR should have a high surface-brightness sensitivity with a spectral resolution of at least 500 Hz; a desirable spectral resolution would be 10 Hz.

**Variable Phenomena** In addition to space-weather studies, LOFAR will be able to observe a variety of objects or phenomena that can have rapid temporal changes, e.g., pulsars, interplanetary scintillation,

extrasolar planet bursts. This requirement also demands high time-resolution capabilities and good instantaneous  $u$ - $v$  coverage.

**Polarization** At LOFAR’s higher frequencies, solar magnetic phenomena, Jupiter, pulsars, and extragalactic sources are expected to display significant polarization. LOFAR will have full polarization capabilities.

**Declination Coverage** Using H II regions to constrain the cosmic-ray distribution and studies of pulsars, SNRs, X-ray binaries, and other discrete Galactic sources require that LOFAR be able to see a significant part of the Galactic plane, especially towards the inner Galaxy. The Galactic center is an especially desirable target for LOFAR observations (Kassim et al. 2003b).

**Field of View** Ionospheric phase fluctuations can be tracked by self-calibration as time-variable contributions to the antenna-based phase solutions. However, if the field of view is larger than the isoplanatic patch, then the time-variable ionospheric phases also acquire an angular dependence. New imaging algorithms (e.g., field-based calibration Cotton & Condon 2002; Kassim et al. 2003a) address this problem and are needed for the 74 MHz VLA where the field of view ( $> 10^\circ$ ) exceeds the isoplanatic patch (often  $< 1^\circ$ ). LOFAR will mitigate this problem by limiting the field of view through hardware design by phasing the signals from closely spaced dipole antenna “elements” into a station, thereby also providing good primary beam definition. If the stations are large enough, the field of view will be limited to less than the typical isoplanatic patch; the Clark Lake TPT array (Erickson et al. 1982) field of view at 74 MHz ( $< 2.5^\circ$ ) was a result of its large stations. Additional restraints on the field of view are provided by bandwidth- and time-averaging effects.

**Ionospheric Compensation** The 74 and 330 MHz VLA systems demonstrate that self-calibration can remove ionospheric phase effects when the full array signal-to-noise ratio is 3–5. As the signal-to-noise ratio on an individual baseline is a factor of  $N^{-1/2}$  smaller than that for an array of  $N$  individual antennas (or dipole stations), an array of roughly 40 stations would mean that a signal-to-noise ratio of approximately 1 would suffice. Considering also the desire for excellent  $u$ - $v$  coverage, the current LOFAR design calls for roughly 100 stations. The robustness of self-calibration can be increased further by dual-frequency ionospheric phase referencing (DFIPR, Kassim et al. 1993): corrections for ionospheric phase fluctuations are measured at a higher frequency and then scaled to a lower frequency. DFIPR increases significantly the coherence time of the data, allowing longer integration times for self-calibration. The possibility of having a concurrent higher frequency ( $> 100 \text{ MHz}$ )

data stream in order to track the ionospheric disturbances at the lower frequencies ( $< 100$  MHz) is naturally afforded by LOFAR’s broad frequency coverage.

## 5. LOFAR: Science Drivers

### 5.1. Science Drivers: Overview

The Low Frequency Array is motivated by a large number of science drivers from a wide range of astronomical fields. Some of the major fields LOFAR would contribute to significantly include but are not limited to: (1) the epoch of reionization (EOR), (2) emission (disk and halo) and absorption mechanisms in galaxies, (3) the search for fossil radio galaxies, (4) supernova remnants and their connection to cosmic-ray acceleration, (5) the physical parameters of H II regions, (6) interstellar propagation effects, (7) carbon recombination lines, (8) the Galactic distribution of cosmic rays (9) pulsars in other galaxies, (10) finding high redshift radio galaxies and (11) the study of cluster radio halos and relics. In the next section we explain in detail the usefulness of LOFAR to last topic mentioned: cluster research.

### 5.2. Science Drivers: Cluster Research

The surface brightness sensitivity and low-frequency capabilities of LOFAR means that it will be an ideal probe of diffuse, steep-spectrum radio sources in clusters of galaxies. Two such classes of sources are known, radio halos and the lobes of radio galaxies.

A small number of galaxy clusters have been found to have radio halos—diffuse, central radio emission not associated with any one galaxy in the cluster (e.g., A754, Kassim et al. 2001). Models for the origins of these halos include injection of relativistic electrons from radio galaxies, turbulent *in situ* particle acceleration, or a merger shock wave and secondary production from hadronic interactions of cosmic ray protons with the intracluster medium (Schlickeiser et al. 1987). The magnetic fields within the halos have been proposed to be the result of phase transitions occurring after the Big Bang, battery effects at shock waves, injection by radio galaxies and galactic winds, or dynamo action driven by structure formation flows. While each model has its advantages, none can explain all of the observed features of radio halos.

Most models predict a much higher number of cluster halos than observed. The “missing” halos may have escaped detection by virtue of their steep spectra, suggesting that a low-frequency search will find many more halos. Many models predict that radio halos are transient, and a pool of relic electrons with energies  $E \sim 100$  MeV is expected due to the long cooling times in this energy range (Sarazin 1999). Indirect evidence for the existence of these relic electrons has been found recently as excess extreme ultraviolet emission from clusters (Hwang 1997; Ensslin & Biermann 1998; Sarazin & Lieu 1998; Bowyer & Berghöfer 1998), emission that may be due to inverse Compton scattering of cosmic background photons (Leiu et al. 1996; Bowyer et al. 1996, 1997; Mittaz et al. 1998). If the radio synchrotron emission from these

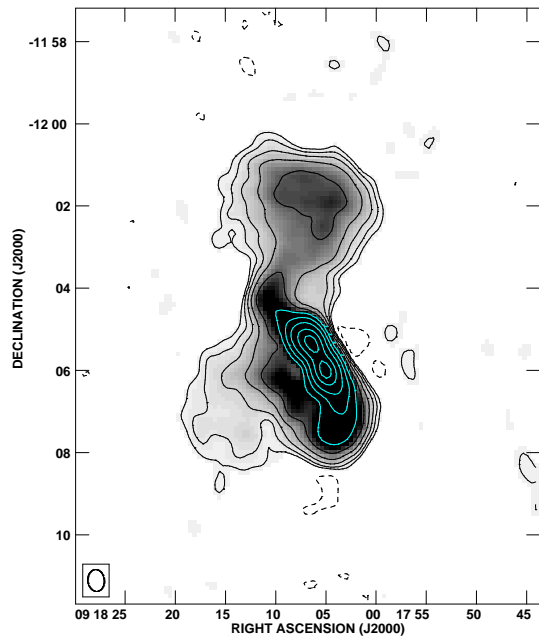


FIG. 7.— Hydra A at 74 MHz. The contours are at multiples of the  $3\sigma$  noise level,  $0.2 \text{ Jy beam}^{-1} \times -1, 1, 2, 4, 8, 16, \dots$ . The image has been corrected for the attenuation of the primary beam.

halos can be detected, the combined radio and EUV information will provide a measurement of the magnetic field strength inside the intracluster medium. An initial comparison for the Coma cluster indicates the existence of highly structured magnetic fields (Ensslin et al. 1999). The combination of the number of halos and magnetic field strength within them will provide more stringent observational constraints for models.

Low radio frequency measurements of polarized background sources are also a sensitive tool for detecting weak magnetic fields outside clusters of galaxies because of the  $\lambda^2$  dependence of Faraday rotation. The high angular resolution and sensitivity of LOFAR may enable it, at the high end of its frequency range, to measure changes in the Faraday rotation across extended, polarized, background sources. The sensitivity of LOFAR will increase the number of background sources that can be used to probe the peripheries of any given cluster and will extend studies of the magnetic fields to the peripheral regions of cluster with good statistics for the first time.

Often sitting in the center of the cluster’s gravitational potential is a large elliptical galaxy containing an active galactic nucleus (AGN). The AGN drives relativistic jets of electrons into its surroundings. Recently, it has become clear that these jets can influence the central cluster properties. The jets inflate “bubbles,” containing synchrotron-emitting plasma that typically are buoyant in the intracluster medium. In some cases, the total amount of energy carried by the jet and deposited in the bubbles can exceed that being radiated in the X-ray (e.g., Virgo A, Fig. 4, Owen et al. 2000). In other

cases, e.g., 3C 84, the AGN may not be heating the intracluster medium as vigorously, yet the buoyant action of the bubbles is nonetheless modifying the intracluster medium, as is apparent in both radio and X-ray observations (Fabian et al. 2002). More recently, Lane et al. (2004) have shown that Hydra A (Fig. 7) also appears to have large radio lobes that could be producing bubbles in its intracluster medium. With its much greater surface brightness sensitivity (based on the number and distribution of stations relative to the VLA antennas), LOFAR should be able to find many more such bubbles, particularly in concert with future X-ray observatories, and trace the extent of the radio emission to larger distances from the center of the cluster.

## 6. Current Status of LOFAR

LOFAR is funded and being developed by an international consortium comprised of the Naval Research Lab-

oratory and MIT's Haystack Observatory in the US, and ASTRON in the Netherlands. A formal management structure is in place, and there are ongoing prototyping activities as well as an active international Science Consortium. The project was recommended by the US National Academy of Science Astronomy Decade Report. There is an ongoing preliminary design review (PDR), with a goal for completion of the array by the end of the decade.

Basic research in radio astronomy at the NRL is supported by the Office of National Research. A portion of this work was performed while A. C. held a National Research Council-NRL Research Associateship.

## References

- Bowyer, S., Lampton, M., & Lieu, R. 1996, *Science*, 274, 1338  
 Bowyer, S., Lieu, R., & Mittaz, J. P. 1997, in *The Hot Universe*, IAU Symp. 188, ed. K. Koyama, S. Kitamoto, & M. Itoh (Kluwer: Dordrecht), 185  
 Bowyer, S. & Berghöfer, T. W. 1998, *ApJ*, 506, 502  
 Clark, T. A., Erickson, W. C., Hutton, L. K., Vandenberg, N. R., Resch, G. M., Broderick, J. J., Knowles, S. H., & Youmans, A. B. 1975, *ApJ*, 80, 923  
 Cotton, W. D. & Condon, J. J. 2002, in *Proc. URSI General Assembly*  
 Ensslin, T. A. & Biermann, P. L. 1998, *A&A*, 330, 90  
 Ensslin, T. A., Lieu, R., & Biermann, P. L. 1999, *A&A*, 344, 409  
 Erickson, W. C., Mahoney, M. J., & Erb, K., 1982, *ApJS*, 50, 403  
 Fabian, A. C., Celotti, A., Blundell, K. M., Kassim, N. E., & Perley, R. A. 2002, *MNRAS*, 331, 369  
 Hwang, C.-Y. 1997, *Science*, 278, 1917  
 Jansky, K. G. in *Proc. I. R. E.*, 23, 1158, 1935  
 Kassim, N. E., Lazio, T. J. W., Erickson, W. C., et al. 2003a, *ApJS*, submitted  
 Kassim, N. E., Lazio, T. J. W., Nord, M., Hyman, S. D., Brogan, C. L., LaRosa, T. N., & Duric, N. 2003b, *Astronomische Nachrichten*, Suppl. I/2003, in press  
 Kassim, N. E., Clarke, T. E., Ensslin, T. A., Cohen, A. S., & Neumann, D. M. 2001, *ApJ*, 559, 785  
 Kassim, N. E., Perley, R. A., Erickson, W. C., & Dwarkanath, K. S. 1993, *AJ*, 106, 2218  
 Kassim, N. E. & Erickson, W. C. 1998, in *Advanced Technology MMW, Radio, and Terahertz Telescopes (SPIE)*, 3357, 740  
 Kronberg, P. P. 1999, private communication  
 Lane, W. M., Clarke, T. E., Taylor, G. B., Perley, R. A., & Kassim, N. E. 2004, *AJ*, in press  
 Lieu, R., Mittaz, J. P. D., Bowyer, S., Breen, J. O., Lockman, F. J., Murphy, E. M., & Hwang, C.-Y. 1996, *Science*, 274, 1335  
 Mittaz, J. P. D., Lieu, R., & Lockman, F. J. 1998, *ApJ*, 498, L17  
 Owen, F. N., Eilek, J. A., & Kassim, N. E. 2000, *ApJ*, 543, 611  
 Perley, R. A. & Erickson, W. C. 1984, VLA Scientific Memorandum 146, National Radio Astronomy Observatory, Socorro, NM  
 Sarazin, C. L. & Lieu, R. 1998, *ApJ*, 494, L177  
 Sarazin, C. L. 1999, *ApJ*, 520, 529  
 Schlickeiser, R., Sievers, A., & Thiemann, H. 1987, *A&A*, 182, 21